Ultimate capacity of undercut fasteners installed in thermally-damaged High-Performance Concrete

P.F. Bamonte & P.G. Gambarova
Department of Structural Engineering, Politecnico di Milano, Milan, Italy

M. Bruni & L. Rossini
MS Engineers, Milan, Italy

ABSTRACT: Medium-capacity metallic undercut fasteners installed in thermally-damaged concrete has been recently the subject of a research project in Milan (∅ = 10 mm = net shank diameter). The results of the third phase of this project, concerning a high-performance concrete (HPC, f_c = 60-65 MPa) are presented in this paper, but the results obtained in the two previous phases are systematically recalled (low-strength concrete-LSC, f_c = 20-25 MPa and normal-strength concrete-NSC, 50-55 MPa). Beside room temperature, five "reference" temperatures (between 200 and 450°C) are considered, to represent as many values of the fire duration prior to the installment of the fastener. The investigation covers four values of the installment depth (h/h_N = 0.45, 0.60, 0.80 and 1.00, where h_N = nominal installment depth = 10∅), and includes the mechanical and thermal characterization of the concrete. In all cases the failure was due to the damaged concrete, with the formation of a conical crack. The systematic formation of this crack was instrumental in formulating a relatively simple model based on limit analysis and on the assumption that the conical crack forms in Mode 1. The model allows to quantify the further loss of capacity that occurs in actual fire situations, where the heating rate is one order of magnitude higher that in the electric furnaces generally used in a lab.

1 INTRODUCTION

Post-installed mechanical fasteners are increasingly used in the prefabrication industry, in most industrial plants, and in a variety of structures and infrastructures often exposed to extreme load situations. As a result of the extensive use of this technology, several valuable technical documents and papers have been published in the last ten years (CEB 1994 & 1997; ACI 2001; Cook et al. 1992; Eligehausen & Ozbolt 1998; Reick 2001; Cattaneo & Guerrini 2004), to allow the designers and the technicians to make the best use of the many types of fasteners available on the market. However, limited attention has been devoted so far to certain severe environmental conditions, like - for instance - high temperature and fire (Eligehausen et al. 2004; Bamonte & Gambarova 2005).

This is the case of tunnels, whose concrete lining may be damaged during a fire, making it necessary to assess the residual capacity of the fasteners after the fire or even to replace the fasteners, to guarantee the safety of suspended pipes (for fresh-air delivery and gas expulsion) and mechanical devices (for electrical and ventilation systems). In both cases, information about the residual capacity provided by the thermally-damaged concrete is a must, since not only the thermal damage in the concrete is irreversible, but may even increase during the cooling phase. On the contrary, the steel shank of a pre-installed fastener recovers most of its original strength after cooling and is mechanically similar to the shank of a newly-installed fastener.

In this research project, medium capacity post-installed non-predrilled undercut fasteners (nominal shank diameter ∅ = 10 mm) are tested, in order to investigate their behavior, after being installed in thermally-damaged concrete (Bamonte & Gambarova 2005). The attention is focused on undercut fasteners, since they are more efficient than expansion fasteners in resisting high temperatures (the bearing action of the concrete is developed farther from the heated surface). Other fasteners, like grouted and adhesive fasteners, should be mentioned as well, but they are non-mechanical devices, and their technology is totally different.

Three concrete grades (f_c = 20-25, 50-55 and 60-65 MPa), 6 reference temperatures (200, 250, 300, 350, 400 and 450°C at the distance $h^* = 8\varnothing_N$ from the heated surface) and 4 installment depths (h = 45, 60, 80 and 100 mm) are investigated, beside room temperature (20°C). Because of the combinations of fastener depth and diameter, fastener failure is mostly controlled by concrete failure and not by shank yielding, except in the virgin concrete.

Other objectives of the project are: (a) the formulation of a relatively-simple limit-analysis model for the description of fastener failure due to concrete fracture (prefixed conical surface, linear crack-opening distribution at the crack interface and cohesive stresses dependent on crack opening); and (b) the definition of a reduction factor to be applied to the ultimate capacity of a fastener installed in slowly-heated concrete, in order to introduce the further damage ensuing from the high thermal gradients caused by an actual fire (fast heating).

During the experimental campaign, a third objective emerged: it became very clear that the well-known C-C Method (Concrete-Capacity Method) (CEB 1994) had to be reformulated in order to explain the extra-capacity of the fasteners installed in the low-grade concrete used in this study (LSC, f_c = 20 MPa), with respect to the fasteners installed in the high-grade concretes used in the first and third phase of this research project (NSC, f_c = 52 MPa and HPC, 65 MPa, see Bamonte & Gambarova 2005).

Sixty fasteners (Figure 1) were post-installed in as many thermally-damaged concrete blocks, simulating 5 values of the fire duration. The ultimate capacity turned out to be a highly-decreasing function of the reference temperature. Preliminarily, the mechanical and thermal properties of the concrete mixes were measured, and the thermal properties were implemented into a FE code, in order to predict the temperature distribution inside each specimen.

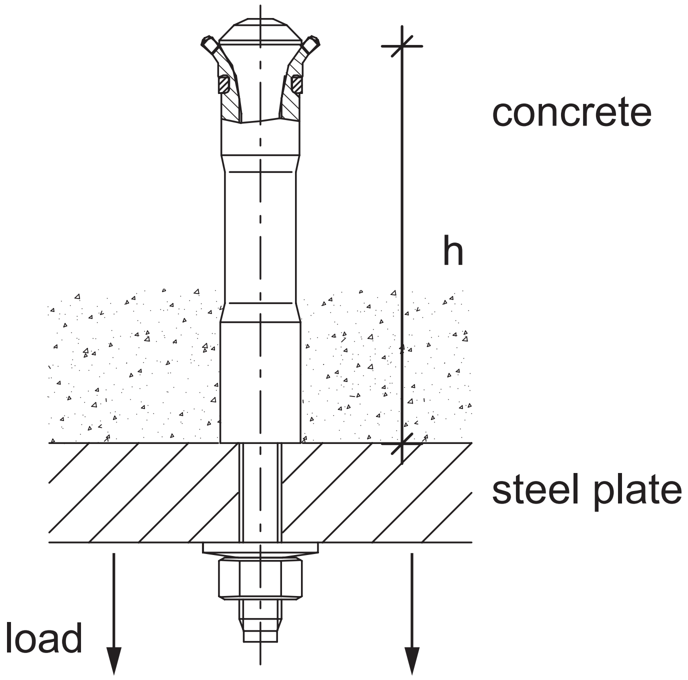

Figure 1. Typical post-installed mechanical fastener, with non-predrilled undercut.

The thermal field was then compared with the temperature values measured inside the first specimen of each concrete grade, by means of a set of thermocouples, and the agreement was very good.

Since the thermal damage in the concrete mostly depends on the maximum temperature reached during the heating process (RILEM 1985; Felicetti & Gambarova 1998; Phan & Carino 2002; Cheng et al. 2004), the residual capacity of a fastener is a good indication of its high-temperature capacity.

As for the formulation of a model to describe the further damage induced by fast heating (as in actual fires), the roughly conical fractures typical of the tests on headed studs indicate a major role for crack opening and cohesion (Mode I: only past the peak load does some slip occur). For such a reason, a simple model based on the transmission of normal stresses is under develop-ment, and the necessary checks are still in progress.

2 EXPERIMENTAL PROGRAM

2.1 *Test philosophy and temperature-related problems*

As already mentioned, this project is focused on non-predrilled undercut fasteners of medium capacity, since this type of fasteners is interesting in terms of fire-sensitivity and pull-out capacity. As a matter of fact, the large depth of large fasteners makes these devices less sensitive to concrete damage, for any reasonable fire duration, while small fasteners are of less importance for their limited capacity. A single diameter was considered (nominal shank diameter $\varnothing_N$ = 10 mm; net diameter $\varnothing$ = 8.6 mm; outside diameter of the whole body $\varnothing_0$ = 18 mm; suggested nominal depth of the drilled hole $h_N = 10\varnothing_N$ = 100 mm).

The effective depth of the fasteners was limited in most cases to $8\varnothing_N$ to represent a situation where the heavily-damaged concrete layer exposed to the fire has been removed after the fire, to be replaced with a new concrete or mortar layer (thickness h_0), that has no structural relevance. In such a case, even if the depth of the fastener is given the nominal value (h_N), the effective depth is smaller ($h = h_N - h_0 = 0.8h_N$ in most of the cases investigated in this study).

The value $h^* = 80\%\ h_N$ (= 80 mm) has thus been adopted as a reference for the maximum temperature reached inside each specimen, and as a criterion upon which comparisons are made between “slow heating” (in the electric furnace) and “fast heating” (typical of both standard fires and real fires). Consequently, in each test reference was made to the temperature reached at the depth h^* (T = 200, 250, 300, 350, 400 and 450°C).

In one specimen of each concrete grade, the temperature profile was monitored by means of 3 thermocouples installed at approximately 25, 80 and 175 mm from the heated surface (specimen thickness = 200 mm, Figure 4). In Figure 2, the diffusivity of the concretes adopted in this study is plotted as a function of the temperature; the measurement of the thermal diffusivity allows to perform numerical simulations to evaluate the temperature profiles at any given heating duration. An example is shown in Figure 3, where the measured temperature profiles in the HPC specimen are compared with the corresponding numerical simulations: note that, although the overall trend of the temperatures is correctly described, sizeable differences are observed at the exposed and unexposed surfaces.

In the following, the thermal profiles used in the interpretation of the test results will be taken from the experimental measures, using a third-degree interpolating function along the depth of the specimen. The numerical simulation will be used only to work out the thermal profiles ensuing from the ISO-834 Fire Curve.

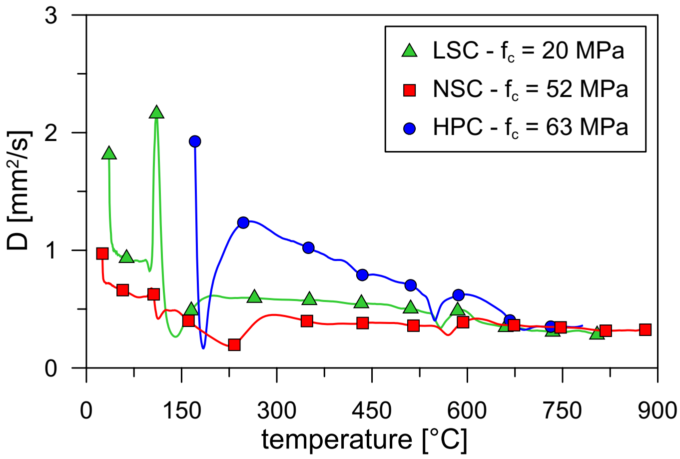

Figure 2. Plots of the thermal diffusivity of the concrete measured in this study and adopted in the analysis.

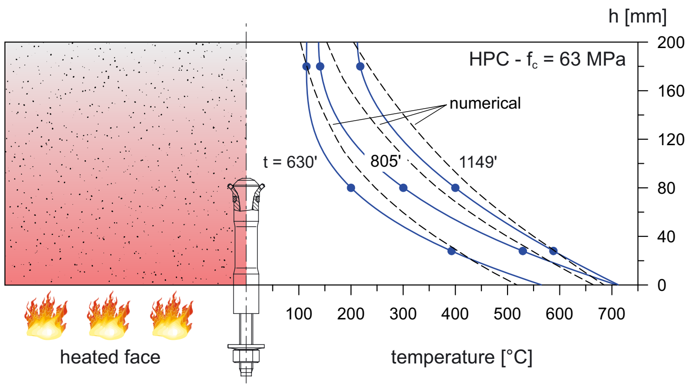

Figure 3. Temperature profiles: measured values (full curves) and thermal analysis (dashed curves) for three different values of the heating duration.

Sixty concrete blocks – or specimens – were cast (Figure 4: dimensions 400 × 400 × 200 mm in 55 blocks and 400 × 300 × 200 mm in the remaining 5 blocks). All blocks were fastened to the front face of the chamber of the furnace (Figure 4), with the door open, in order to have one of the face of the specimen exposed to high temperature. After the cooling process, a hole was drilled in the centroid of the

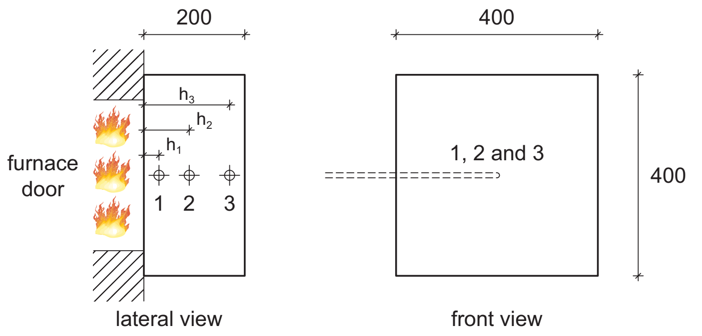

Figure 4. Typical preliminary specimen used to determine the temperature distribution inside the concrete blocks.

Figure 5. Loading rig during a typical pull-out test.

heated face of each specimen, up to the required depth. Then the fastener was installed and tested in the next few days (maximum one week past the cooling). The loading set-up was a simple steel rig (Figure 5) consisting of a loading ring, three inclined legs, a reaction plate and a hydraulic actuator. One LVDT was used to measure the displacement of the fastener with respect to the undisturbed concrete mass, and to control the test. All tests were displacement-controlled, and the displacement rate was ds/dt = 0.5 mm/min (1.0 mm/min in the final part of the test, at the end of the softening branch).

In each case (corresponding to a given couple of values of the reference temperature and of the installment depth), at least two nominally-identical specimens were tested for repeatability.

The diagrams of concrete mechanical and physical properties are plotted in Figs. 6 and 7 (cylindrical compressive strength, direct tensile strength, stabilized elastic modulus, mass per unit volume and fracture energy) as a function of the temperature.

With reference to the fracture energy (Fig.7), only two reference temperatures were considered in the case of low-strength concrete (T = 20 and 350°C, for want of specimens, Fig.7b), compared to 5 values in the case of high-performance concrete (T = 20, 200,

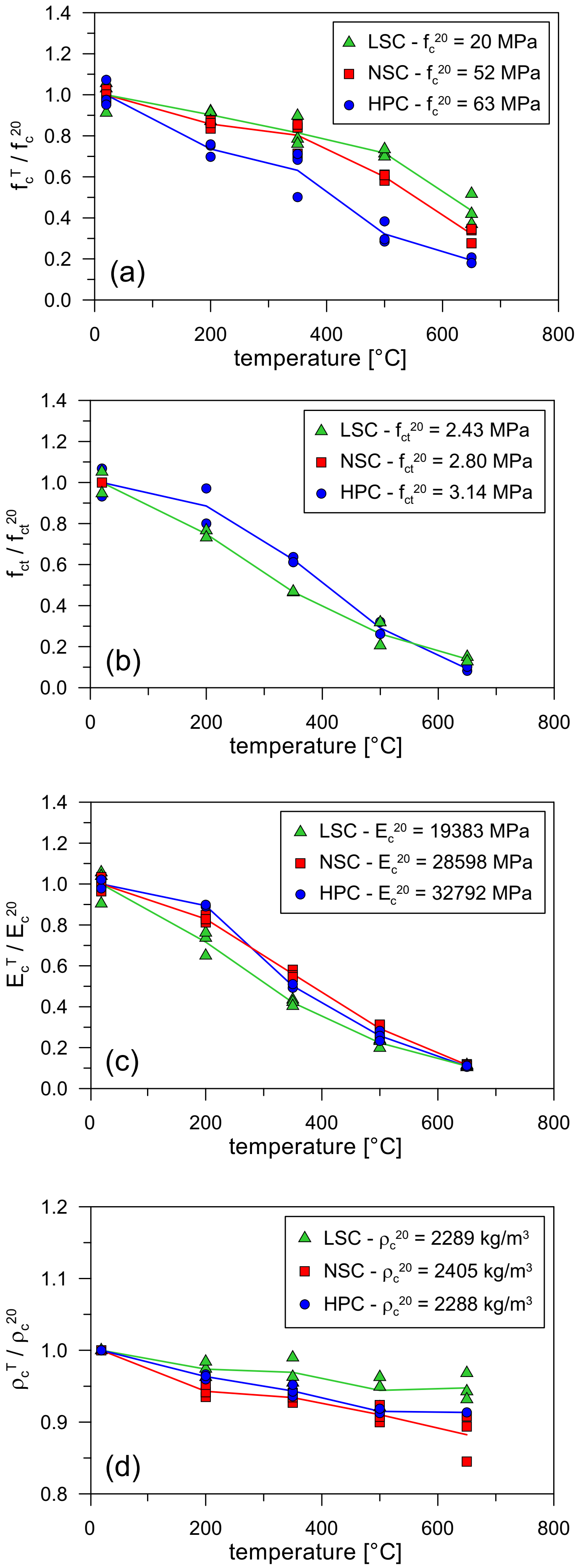

Figure 6. Residual mechanical and physical properties as a function of the temperature: (a) cylindrical compressive strength; (b) direct tensile strength; (c) stabilized elastic modulus; and (d) mass per unit volume.

350, 500 and 600°C, Figure 7b). The direct tensile strength (f_{ct}) was evaluated by multiplying the indirect tensile strength measured in three- (LSC) or four-point bending (HPC) ($f_{ct,fl}$: size of the prisms 600 × 150 × 150 mm) by the size-dependent factor $\{[1.5\cdot(h/h_o)^{0.7}]/[1 + 1.5\,(h/h_o)^{0.7}]\}$, where h is the actual depth of the section of the prisms and h_o = 100 mm is a reference depth (MC90). The fracture energy was evaluated as the area enveloped by the load-displacement curve minus the energy dissipated during nonlinear cracking phenomena taking place during the loading phase prior to the attainment of the maximum load (Figure 7a). Contrary to the other mechanical properties, fracture energy increases up to 300-400°C and then starts decreasing (at 500-600°C the values are very close to those in the virgin conditions, see also Zhang & Bicanic 2002).

2.2 *Test results*

Considering the various parameters coming into play and the difficulties encountered during the experimental campaign, it was possible to perform a total

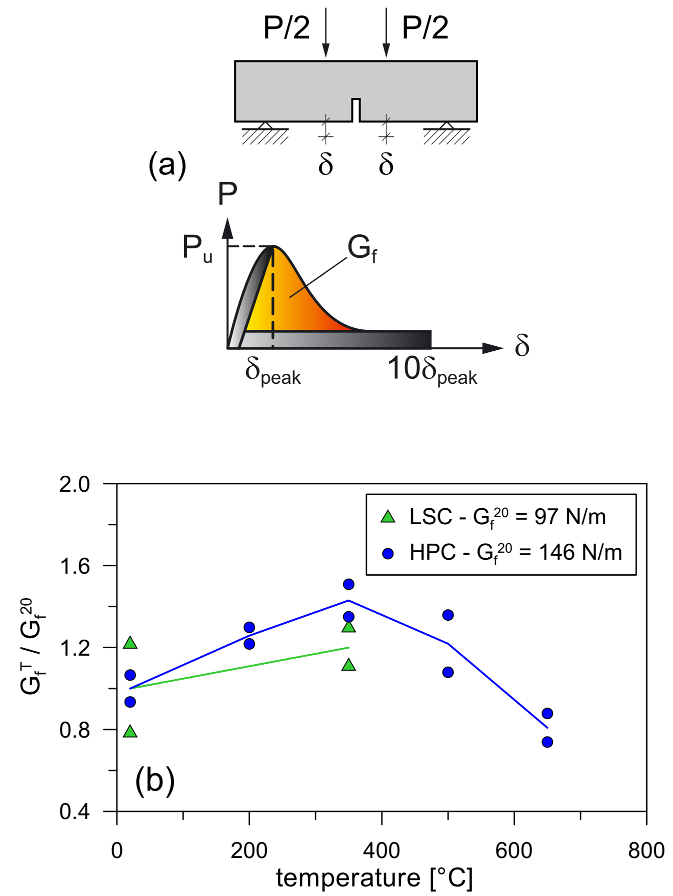

Figure 7. Residual fracture energy as a function of the temperature: (a) calculation procedure; and (b) test results.

of 60 successful tests, Specimen's failure was always controlled by concrete fracture in the thermally-damaged specimens and in LSC virgin specimens, while NSC and HPC virgin specimens failed because of shank yielding. (In NSC and HPC virgin specimens, the ultimate load ensuing from concrete fracture was evaluated by means of the CC* method, as explained in the following). As a rule, two nominally-identical specimens were tested in each case for repeatibility, except in one case, where the scattering of the test results required a third test.

In most cases a clear-cut conical fracture occurred, with and without thin radial cracks (Bamonte et al. 2006). In some cases, the conical fracture was accompanied by the subdivision of the specimen into 2-4 blocks, but in most of these cases the overall cracking was the result of the simultaneous formation of the conical crack and of cross-shaped radial cracks, as if the two mechanisms were activated at the same time. Moreover, the formation of these cracks and of the ensuing failure mechanism was observed after the attainment of the peak load: thus, it is reasonable to assume that the bearing capacity of the different specimens was not affected by the evolution of cracking past the peak load and specifically by the radial cracks, that appeared only in the final stage of the loading process.

2.3 *Interpretation of the test results at 20°C*

A number of preliminary tests at room temperature were performed, for different values of concrete grade and embedment depth, in order to study the influence of the different parameters coming into play. As it is well known, the original C-C Method is based on the following formulation for the ultimate capacity:

$$P_u = k_1 f_c^{\,0.5} h^{1.5} \qquad (1)$$

Eq.(1) is valid for a given family of concretes, since all the parameters (maximum aggregate size d_a, aggregate type, cement type and content, hydraulic adjuncts, …) are lumped into a single coefficient (k_1).

However, if different mixes are to be compared as in this project, with very different fracture properties, the C-C Method proves to be inadequate, and Eq.(1) should be reformulated. In the following, in Eq.(1) the tensile strength of the concrete ($f_{ct} \approx f_c^{0.5}$) is replaced by the fracture energy G_f, that is given the formulation proposed in MC90 (1991):

$$G_f = 0.2 \cdot \left(10 + 1.25 d_a\right) f_c^{\,0.7} \qquad (2)$$

By introducing the fracture energy it is possible to take care of the maximum aggregate size (d_a) that controls crack roughness and cohesion:

$$P_u = k_2 G_f h^{1.5} \qquad (3)$$

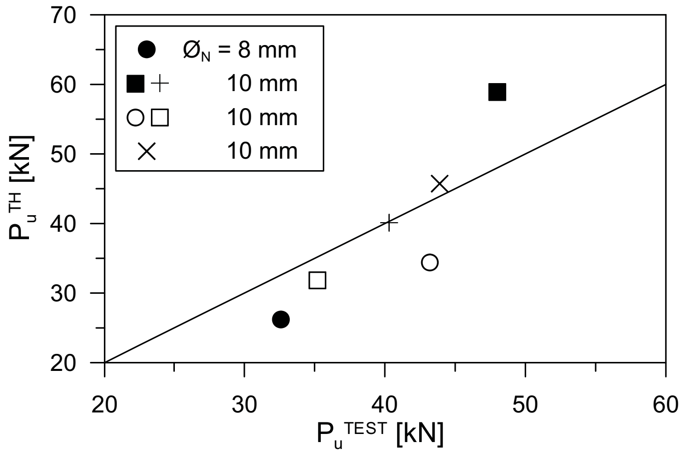

Figure 8. Fitting of the test results at 20°C by means of the proposed reformulation of the CC-Method (CC*-Method, Eq.(3))

where k_2 is a parameter whose value mostly depends on fastener type (k_2 = 1.01 is the mean value in the tests carried out by the authors and by Eligehausen & Ozbolt 1998). Note that Eqs.(1) and (3) take care of the so-called size effect ($\approx h^{-0.5}$, CEB 1997; Eligehausen & Ozbolt 1998). Since the pull-out of the fasteners (except in the case of shank yielding) is controlled by concrete fracture, introducing concrete fracture energy in the formulation of the pull-out load looks very reasonable, as shown by the somewhat better agreement between the test results and the theoretical predictions. (However, a rather large scattering cannot be ruled out, since parameters other than d_a and f_c come into play).

Moreover, in Eq.(3) the possible advantage of explicitly introducing the aggregate is weakened by the enhanced dependence on the compressive strength compared to Eq.(1). A further improvement could be the explicit introduction of the role of the aggregate size by means of the bilinear expression contained in Eq. (2), together with the dependence on the square root of the compressive strength, as in Eq. (1).

Table 1. Main parameters of the tests at 20°C considered in Figure 8 for the evaluation of the parameter k_2 in eq.(3).

	h [mm]	d_a [mm]	f_c [MPa]	author
🖃	60	22	26	Eligehausen et al.
+	65	19	27	prelimary test
🖂	65	20	52	NSC, 1st phase
☎	60	19	27	preliminary test
🖅	60	28	20	LSC, 2nd phase
×	45	25	63	HPC, 3rd phase

In Figure 8 the results obtained in this project at 20°C (1st, 2nd and 3rd phases), some test results by other authors and the values of the ultimate capacity predicted by Eq.(3) are compared for d_a = 19-28 mm, f_c = 20-63 MPa.

All the test results obtained in this study are gathered together in Figure 9, that clearly shows that the failure mode is markedly affected by the temperature. Even if in the virgin specimens (T = 20°C), at

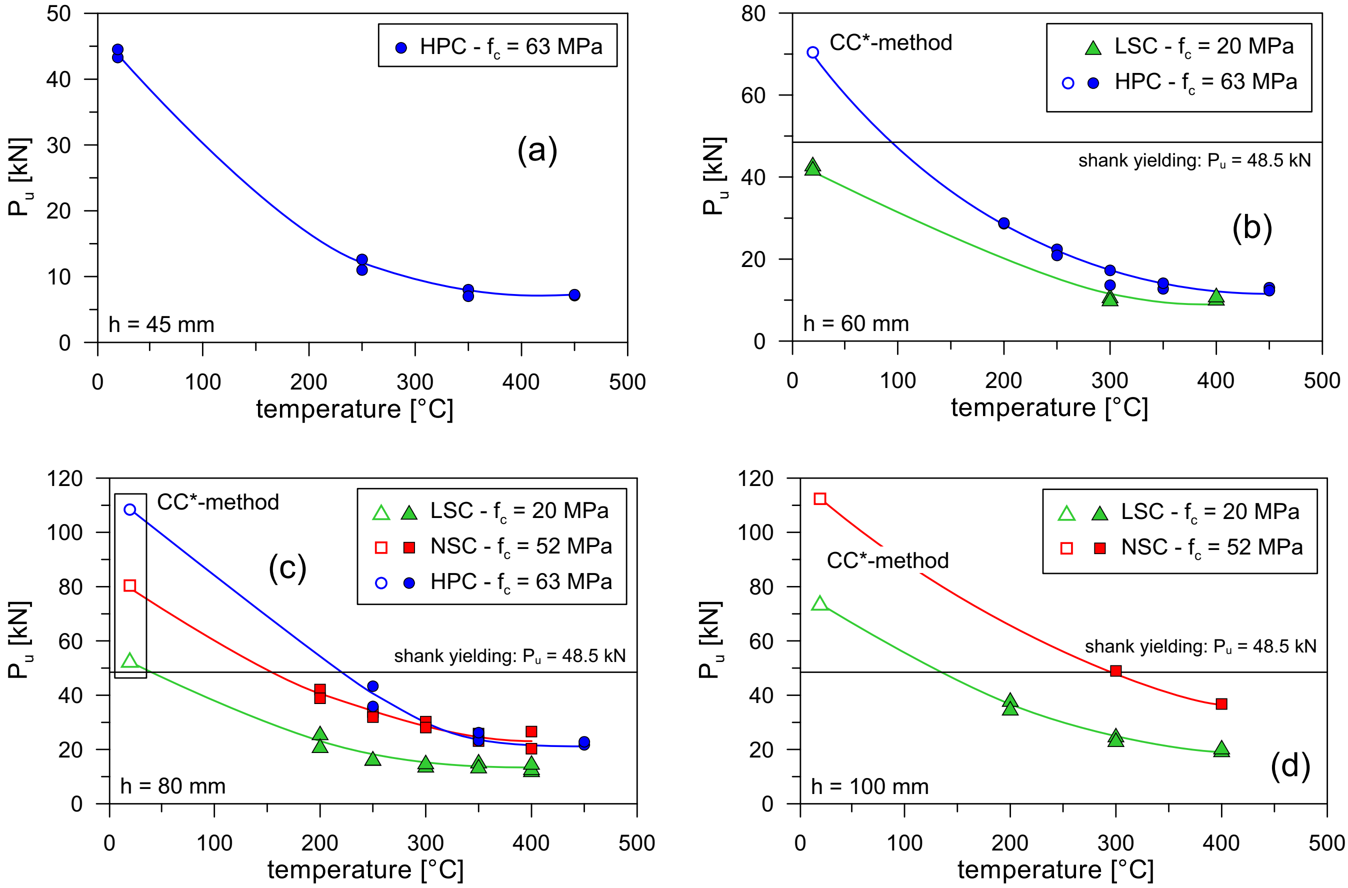

Figure 9. Residual pull-out loads as a function of temperature: (a) h = 45 mm; (b) h = 60 mm; (c) h = 80 mm; and (d) h = 100 mm.

medium and large installment depths, and for the highest-grade concretes, the pull-out failure is caused by shank yielding, the ultimate load-temperature curves show a regular descending trend, a marked "flattening" above 300°C and a tendency towards a smaller role for concrete strength with increasing temperature (there are marginal differences between NSC and HPC above 250°C, Fig.9c, and limited differences between LSC and HPC above 300°C, Fig.9b).

For instance, Figure 9c shows that after reaching 400°C at $h/h_N = 0.8$, the pull-out capacity is roughly 1/5 of the capacity of the virgin specimens - if reference is made to concrete fracture -, and from 1/5 (LSC) to 1/3 (NSC and HPC) - if reference is made to shank yielding.

As previously observed in Bamonte & Gambarova (2005) with reference to the C-C Method, both the C-C Method and the Modified C-C Method (C-C*) are totally unable to describe the mechanical decay of fasteners installed in thermally-damaged concrete. Of course, the average temperature of the concrete between the head of the fastener and the heated surface should be introduced, but even in this case the aforementioned models tend to overestimate the capacity of a fastener by up to 3 times.

There are at least two reasons: firstly the tensile strength is more affected by the temperature than the compressive strength, and secondly the thermally-induced microcracks tend to damage the crack interface to the detriment of the roughness induced by the aggregates. However, further tests and deeper studies are needed, since concrete fracture energy is an increasing function of the temperature up to 300°C (Figure 7).

2.4 *High and low heating rates*

The heating rate in an electric furnace generally does not exceed 10-15°C/minute, which is an order of magnitude less than in real fires. Consequently, an answer should be given to the question to what extent the capacity measured under low heating rates (as in the tests performed in this project) is overestimated compared to that under high heating rates.

In order to compare the ultimate capacities of a fastener installed in a slowly-heated or rapidly-heated concrete block, a theoretical model is under development, with the following assumptions:

(a) the ultimate capacity is reached when the opening of the conical crack has the critical value under the head and zero value along the heated surface; as a matter of fact, the fitting of the test results shows that the ultimate resis-

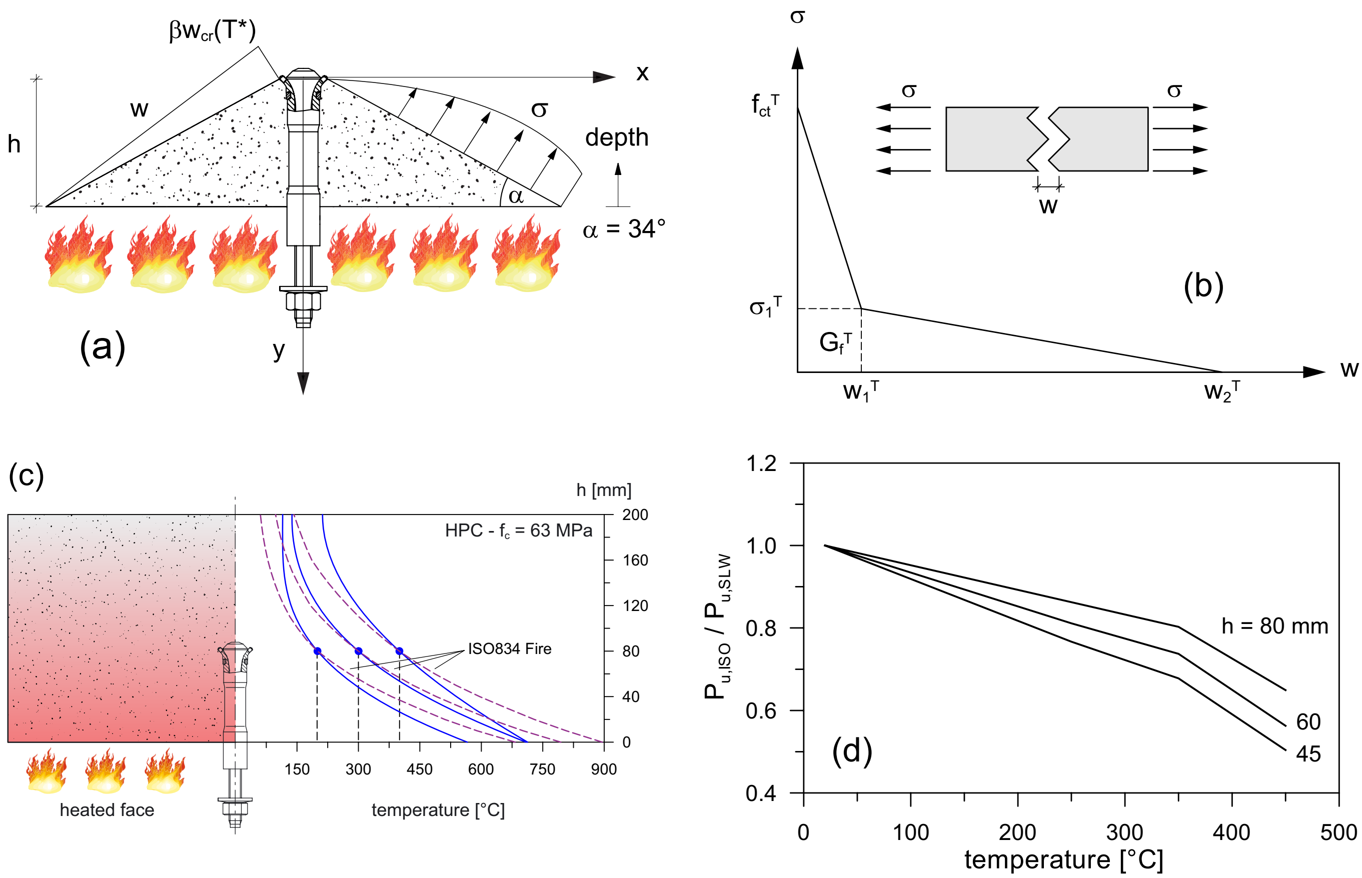

Figure 10. (a) Limit analysis model; (b) bilinear softening law in tension; (c) temperature profiles for fast heating (ISO 834, dashed curves) and slow heating (these tests, continuous curves), for the same temperature at the reference depth (h^* = 80 mm, T = 200, 300 and 400°C); and (d) ultimate capacity under fast heating normalized to that under slow heating, as a function of the temperature (HPC).

tance is reached before the attainment of the critical value w_{cr}^T under the head. The coefficient β takes care of such fact (β = 0.25 for LSC; = 0.15 for NSC and = 0.05 for HPC). Since for β = 0 there is no softening, β may be considered as a “toughness parameter” (as it is well known, the lower the grade, the greater the toughness for the same aggregate size);

(b) the profile of the opening is linear (see “w” in Figure 9a);

(c) the stress-crack opening law of the material is a bilinear decreasing function, where the tensile strength and the fracture energy are a function of the temperature (Figure 10b; $\sigma_1^T = f_{ct}^T/4, w_1^T = 0.75G_f^T/f_{ct}^T, w_2^T = 5G_f^T/f_{ct}^T$);

(d) the fracture energy is variable with the temperature;

(e) the pull-out force is the integral of the cohesive stresses transmitted at the crack interface, where the local stress is related to the local crack width, through the temperature-dependent stress-crack width law.

The temperature profiles (Figure 10c) and the ensuing temperature values along the conical crack in the case of a standard ISO-834 Fire were evaluated by means of numerical simulations, taking advantage of the diffusivity measured in the preliminary tests (Figure 2). The criterion used to compare the exposures to fires of different heating rates was the temperature reached at the reference depth of h^* = 80 mm. With reference to HPC (f_c = 63 MPa), Figure 10c shows the temperature profiles in the case of a slow-heating process (continuous curves) compared to the temperature profiles ensuing from standard ISO-834 Fire (dashed curves).

Modeling the various situations (h = 45, 60, 80 mm, low heating rate and standard ISO-834 fire), leads to the curves shown in Figure 10c, where the ratio between the capacity after a standard fire and that after a slow heating process is plotted as a function of the reference temperature reached at the depth h^*. For T = 400°C, the capacity after the standard fire is 75%, 65% and 60% of the capacity after a slow heating, depending on the installment depth (h = 80, 60, 45 mm).

3 CONCLUDING REMARKS

In spite of the limits set by the technology used in the tests and by the choice of the specific fasteners adopted in this project, some general remarks can be formulated, to help producers, designers and technicians in their day-to-day activity aimed at structural safety:

- Mechanical undercut fasteners installed in thermally-damaged concrete exhibit a strong temperature sensitivity, that seems to be larger in low-grade concretes than in high-grade concretes.

• The residual ultimate capacity markedly depends on the effective depth, since the larger the installment depth, the less damaged the concrete underneath the head of the fastener. For example, in the medium-capacity fasteners investigated in this study, embedded in a high-performance concrete, the temperature of 220°C at the reference depth $8\varnothing_N$ turns the failure mode from shank yielding to concrete fracture, while the same occurs at less than 100°C at the effective depth $6\varnothing_N$.

• The Concrete-Capacity Method - extensively used when fasteners have different depths and are installed in similar virgin concretes differing only for the compressive strength – tends to grossly overevaluate the residual capacity, if concrete compressive strength is given the value corresponding to the temperature reached underneath the head of the fastener or to the mean temperature value between the head and the heated surface. Even the Modified Concrete-Capacity Method based on concrete fracture energy proves to be largely inadequate.

• There is a strong correlation between the residual capacity after a slow heating process (typical of the electric furnaces used in a laboratory) and the fast heating process associated with the standard fire. The latter situation leads to definitely-lower capacities. However, slow heating processes are instrumental in avoiding concrete spalling in a lab. For instance, after reaching 350°C at the reference depth $h = 0.8\ h_N$, depending on the actual fastener depth the capacity during the standard fire is from 44% to 66% of that under slow heating for the high-performance concrete investigated in this study.

4 ACKNOWLEDGEMENTS

The financial support by Italcementi Group – C.T.G. (Bergamo, Italy) and the supervision of CIS-E (Int. Center for the Constructions in Europe) are gratefully acknowledged (Research Project "Experimental and Theoretical Investigation on the Mechanical Behavior of Post-Installed Undercut Fasteners Installed in Thermally-Damaged Plain and Fiber-Reinforced High-Performance Concretes", March 2004).

The technicians Antonio Cocco and Paolo Broglia of the Laboratory for Building Materials should also be praised for their commitment to the success of this project.

REFERENCES

ACI. 2001. Evaluating the Performance of Post-Installed Mechanical Fasteners in Concrete and Commentary. ACI 355.2/ACI 355.2R, Concrete International, February 2001: 106-136.

Bamonte, P. & Gambarova, P.G. 2005. Residual Behavior of Undercut Fasteners Subjected to High Temperatures. Proc. of the International fib Symposium "Keep Concrete Attractive", edited by Balázs G, Borosnyói A, May 2005, Budapest (Hungary); Vol.2: 1156-1163.

Bamonte, P., Gambarova, P.G., Gorla, A. & Niglia, A. 2006. Residual Capacity of Undercut Fasteners Installed in Thermally-Damaged Concrete. Proc. of the 2nd International fib Congress, June 2006, Naples (Italy), Vol.1; 234-235 (12-page paper on CD).

Cattaneo, S. & Guerrini, G. 2004. Mechanical Fasteners Installed in High-Performance, Fiber-Reinforced Concrete (in Italian). Proc. of the National Conference of the Italian Society for R/C and P/C Structures – AICAP, May 2004, Verona (Italy): 101-112.

CEB-FIB Model Code 1990. Thomas Telford ed., London, 1991.

CEB. 1994. Fastenings to Concrete and Masonry Structures. State-of-the-Art Report, Bulletin d'Information No. 216, Thomas Telford ed., London.

CEB. 1997. Design of Fastenings in Concrete. Design Guide – Parts 1,2,3, Bulletin d'Information No. 233, Thomas Telford Ed., London.

Cheng, F.P., Kodur, V.K.R. & Wang, T.C. 2004. Stress-Strain Curves for High Strength Concrete at Elevated Temperatures. ASCE Journal of Materials in Civil Engineering; 16(1): 84-90.

Cook, R.A., Collins, D.M., Klingner, R.E. & Polyzois, D. 1992. Load-Deflection Behavior of Cast-in-Place and Retrofit Concrete Anchors. ACI Structural Journal; 89(6): 639-649.

Eligehausen, R. & Ožbolt, J. 1998. Size Effect in Design of Fastenings. Special Volume on "Mechanics of Quasi-Brittle Materials and Structures", edited by Pijaudier-Cabot G, Bittnar Z, Gérard B, HERMES, Paris: 95-118.

Eligehausen, R., Kožar, J., Ožbolt, J. & Periskic, G. 2004. Transient Thermal 3-D FE Analysis of Headed Stud Anchors Exposed to Fire. Proc. of the International Workshop "Fire Design of Concrete Structures: What now? What next?", edited by Gambarova PG, Felicetti R, Meda A, Riva P, December 2004, Milan (Italy): 185-198.

Felicetti, R. & Gambarova, P.G. 1998. Effects of High Temperature on the Residual Compressive Strength of High-Strength Siliceous Concretes, ACI Materials Journal; 95(4): 395-406.

Phan, L.T. & Carino, N.J. 2002. Effects of Test Conditions and Mixture Proportions on Behavior of High-Strength Concrete Exposed to High Temperatures. ACI Materials Journal; 99(1): 54-66.

Reick, M. 2001. Fire Behavior of Fasteners Embedded in a Concrete Mass and Subjected to a Pull-out Force. PhD Dissertation, News of the Dept. of Building Materials - IWB; V.2001/4, University of Stuttgart, 166 pp.

RILEM-Commitee 44-PHT. 1985. Behavior of Concrete at High Temperatures. Edited by Schneider U, Department of Civil Engineering, Gesamthochschule Kassel, Kassel (Germany), 122 pp.

Zhang B. and Bicanic N. 2002. Residual Fracture Toughness of Normal- and High-Strength Gravel Concrete after Heating to 600°C, ACI-Materials Journal, V.99, No.3, pp. 217-226.